Theoretical and practical validation tests for a Near-Field to Far-Field transformation algorithm using spherical wave expansion

Eduardo Javier Páez[1], Juan Pedro Regina[2], María Daniela Sandoval[2], Paulino Del Pino[2], Ciro Daniel Tremola[1], Barón Marco Azpúrua[1]

[1]Instituto de Ingeniería. Campo tecnológico de Sartenejas, Carretera Nacional Baruta-Hoyo de la Puerta, Urbanización Monte Elena II. Sartenejas, Baruta 1040-A, Venezuela. epaez@fii.gov.ve , ctremola@fii.gov.ve , bazpurua@fii.gov.ve

[2]Universidad de Carabobo, Venezuela. jpreginag@gmail.com, marysg87@hotmail.com, pdelpi@uc.edu.ve

Abstract

The use of spherical wave expansion of the solution of the wave equation to predict Far-Field values from data measured in the Near-Field region is a well known technique, typically used to perform antenna measurements in compact anechoic chambers. However, when designing the computing algorithm it is fundamental to validate the results and to quantify the numerical error of the method. In this regard, a computer application that samples the electric Near-Field and calculates the values of the electric Far-Field region using spherical wave expansion was developed to measure antenna radiation patterns in the Fresnel zone inside a fully anechoic chamber. In order to validate the code, this paper describes three validation methods: firstly, using the theoretical electric Near-Field values of an infinitesimal dipole as the input to the algorithm to compare the output with the response analytically expected; secondly, using a Far-Field electric field data of a calibrated half wavelength dipole measured in an anechoic chamber and finally, using an electric Near-Field data of a calibrated half wavelength dipole measured in the same chamber. These methods provide simple procedures to calculate the error introduced by the code in different scenarios that should be considered to estimate the measurement uncertainty.

Keywords: near-field far-field, numerical transformation, spherical wave expansion, antenna radiation pattern, anechoic chamber.

Ensayos de validación teóricos y prácticos para un algoritmo de transformación de medidas en campo cercano a campo lejano usando la expansión de ondas en coordenadas esféricas

Resumen

El uso de la expansión de la solución de la ecuación de onda en coordenadas esféricas es una técnica bien conocida para la caracterización de antenas dentro de cámaras anecoicas compactas. Sin embargo, al diseñar el algoritmo de cómputo, es fundamental validar los resultados y cuantificar el error numérico del método. Para ello, se desarrolló un código que calcula el campo eléctrico radiado a partir de las muestras de campo eléctrico en la zona de Fresnel utilizando expansión de ondas en coordenadas esféricas, permitiendo estimar el patrón de radiación. La validación del código se realiza de tres maneras: primeramente, se utilizan los valores de campo eléctrico cercano generado por un dipolo infinitesimal calculados

analíticamente, para compararse luego los resultados de dicho algoritmo con los valores de campo lejano de la antena obtenidos por su expresión analítica; en segundo lugar, se mide el campo eléctrico en zona lejana de un dipolo de media onda calibrado, se utilizan dichos valores como entrada al programa y la salida se compara con la entrada utilizada; y, finalmente, se mide el campo eléctrico en zona cercana de un dipolo de media onda calibrado, se determina el campo lejano con el algoritmo y los valores resultantes se comparan con las mediciones de la misma antena en campo lejano. Estas pruebas permitieron calcular el error introducido por el código en escenarios diferentes, los cuales ayudan a estimar la incertidumbre de la medición.

Palabras clave: campo cercano-campo lejano, transformación numérica, cámara anecoica, expansión de ondas en coordenadas esféricas, patrón de radiación.

1. Introduction

Near-Field (NF) antenna measurement systems have emerged as a reliable alternative to antenna measurement techniques in the Far-Field (FF). Basically, the method consists in measuring the power radiated by the antenna in the Near-Field region, and converting these samples to Far-Field using mathematical transformation techniques (NF-FF). The selection of the most appropriate technique for the NF-FF transformation depends in most cases of practical considerations of measurement systems. For those compact anechoic chambers in where multi-axial positioning systems are used to rotate the antenna in a spherical coordinate system, it is recommend using the Spherical-Wave Expansions technique.

In the 70s, Ludwig used the Spherical-Wave Expansions as a numerical technique to express fields in any region of space [1]. That approach included 99.9% of the radiated power for the calculation of maximum wave order, resulting in Far-Field distributions corresponding to the Near-Field (NF) theoretical synthesized. Thus, it was concluded that the proposed technique was adequate to transform data from Near-Field to the Far-Field region or viceversa. Subsequently, it was found that the major sources of experimental error occur when measurements are taken in the nearby area. Therefore, it was suggested that it should be considered probe's compensation and the Nyquist theorem to establish the spacing between the points of the sampling grid of electric field [2-4].

Years later, it was proposed an alternative method for Near-Field to Far-Field transformation using spherical coordinates. The main contribution of this technique was a pseudo-Green function which, when pre-computed and stored in a database, enables the software to run without major computational requirements [5].

Based upon those previous worηs, a computer application that samples the electric Near-Field and calculates the values of the electric Far-Field region using the spherical wave expansion technique was developed to measure antenna radiation patterns in the Fresnel zone inside a fully anechoic chamber. Our research ends with the validation test made of to verify the proper functioning of the algorithm and to quantify the numerical error in the results.

2. Field regions

The space surrounding an antenna is usually subdivided into three regions, as shown in Figure 1. The inner zone, $r<r_0$, is known as the Reactive Near-Field region, the intermediate one, $r_0<r<r_1$, is called Radiating Near-Field or Fresnel region and the last one is known as the Far-Field region or the Fraunhofer zone. These regions are so designated to identify the field structure in each one. Although no abrupt changes in the field configurations are noted as the boundaries are crossed, there are distinct differences among them. The boundaries separating these regions are not unique, although various criteria have been established and are commonly used to identify the regions [6].

In that sense, the most commonly used criteria to calculate r_0 is given by,

$$r_0 = 0.62\sqrt{\frac{D^3}{\lambda}} \quad (1)$$

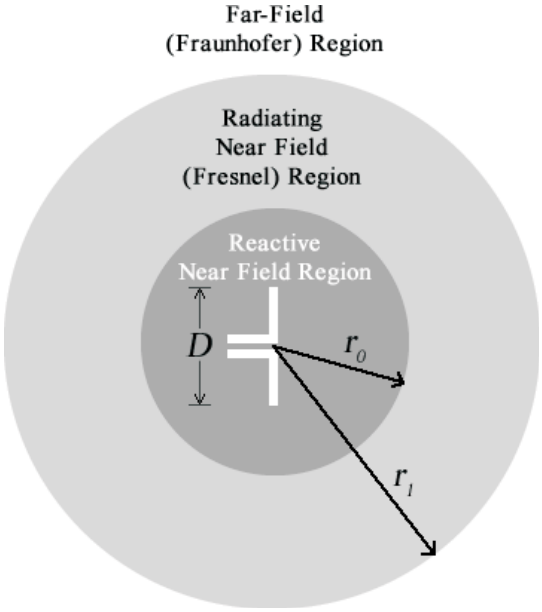

Figure 1. Field regions of an antenna.

Nevertheless, there are also other two criteria to determine $r_{0,}$ which are Polk's criteria (2) and Kay's criteria (3):

$$r_0 = 0.3977\sqrt[3]{\frac{D}{\lambda}}, \text{ and,} \tag{2}$$

$$r_0 = 0.5D\sqrt[3]{\frac{D}{\lambda}} \tag{3}$$

where, D is the largest dimension of the antenna and λ is the wavelength.

Similarly, to estimate the Far-Field Boundary, r_1, some authors have established, introducing a phase error of $\pi/8$:

$$r_1 = 2\frac{D^2}{\lambda} \tag{4}$$

However, this is only true for antennas where $D>>\lambda$ and for free space propagation. For very small antennas is preferable to use:

$$r_1 = 20\lambda \tag{5}$$

$$\text{or, } r_1 = 50D \tag{6}$$

As a general rule, the far field distance is given by

$$r_1 = \max\left(\left\{2\frac{D^2}{\lambda}, 20\lambda, 50D\right\}\right) \tag{7}$$

It is important to notice that in the Far-Field region the field components are essentially transverse and the angular distribution is independent of the radial distance where the measurements are made. This explains why all the conventional antenna measurements and calibrations should be performed in the Fraunhofer zone [6].

3. Spherical wave expansion

It has been shown [1, 7, 8] that any electromagnetic field distribution in a medium homogeneous, isotropic, linear and free of sources, can be expressed in terms the following equations,

$$\mathbf{E} = -\sum_m \sum_n \left(a_{\substack{e_{m,n} \\ o}} \mathbf{M}_{\substack{e_{m,n} \\ o}} + b_{\substack{e_{m,n} \\ o}} \mathbf{N}_{\substack{e_{m,n} \\ o}} \right), \text{ and,} \tag{8}$$

$$\mathbf{H} = \frac{\kappa}{j\omega\mu} \sum_m \sum_n \left(a_{\substack{e_{m,n} \\ o}} \mathbf{M}_{\substack{e_{m,n} \\ o}} + b_{\substack{e_{m,n} \\ o}} \mathbf{N}_{\substack{e_{m,n} \\ o}} \right), \tag{9}$$

where m and n are naturals subscripts used in **M**, **N** and the associated Legendre function, the subscripts e and o represents the even and the odd components of the **M** and **N** vectors and of the coefficients a and b, and refer to the choice of the upper or lower sin(ϕ) or cos(ϕ) dependence. **M** and **N** are auxiliary vector fields, which are solutions of vector wave equation in spherical coordinates, as given by Ludwig [1]:

$$\mathbf{M}_{\substack{e_{m,n} \\ o}} = \mp h_n^{(2)}(\kappa r) \frac{mP_n^m(\cos\theta)}{\sin\theta} \begin{matrix} \sin m\phi \\ \cos m\phi \end{matrix} \mathbf{a}_\theta - h_n^{(2)}(\kappa r) \frac{\partial P_n^m(\cos\theta)}{\partial\theta} \begin{matrix} \cos m\phi \\ \sin m\phi \end{matrix} \mathbf{a}_\phi \tag{10}$$

$$\mathbf{N}_{\substack{e_{m,n} \\ o}} = \frac{1}{\kappa r}\frac{\partial}{\partial r}\left[rh_n^{(2)}(\kappa r)\right] \frac{\partial P_n^m(\cos\theta)}{\partial\theta} \begin{matrix} \sin m\phi \\ \cos m\phi \end{matrix} \mathbf{a}_\theta \pm \frac{1}{\kappa r}\frac{\partial}{\partial r}\left[rh_n^{(2)}(\kappa r)\right] \frac{mP_n^m(\cos\theta)}{\sin\theta} \begin{matrix} \cos m\phi \\ \sin m\phi \end{matrix} \mathbf{a}_\phi \tag{11}$$

where $P_{nm}(\cos\theta)$ is the associated Legendre function, $h_n^{(2)}(\kappa r)$ is the Hankel function of second

class and $\kappa=2\pi/\lambda$, represents the propagation constant.

In the most general case, it should be used a linear combination of the even and odd terms in (8) and (9) but when there is symmetry in the azimuthal axis of the measured electric field, then the expansion can be made only based on even terms or odd terms.

The values of weighted coefficients a and b are determined in terms of the tangential electric field measured in Near-Field, $\mathbf{E_{nf}}$, within a sphere of radius $r_0<r_{nf}< r_1$, that contains all sources, and **M** and **N** vector fields evaluated at the same radius [1, 9, 10].

$$a_{\substack{e_{m,n}\\o}} = \frac{1}{\left[h_n^{(2)}(\kappa r_1)\right]^2}\frac{2n+1}{2\pi n(n+1)}\frac{(n-m)!}{(n+m)!}\times \int_0^{2\pi}\int_0^{\pi} -\mathbf{M}_{\substack{e_{m,n}\\o}}\mathbf{E_{nf}}(r_1,\theta,\phi)\sin\theta d\theta d\phi \quad (12)$$

$$b_{\substack{e_{m,n}\\o}} = \frac{1}{\left[\frac{1}{\kappa r_1}\frac{\partial}{\partial r}\left(r_1 h_n^{(2)}(\kappa r_1)\right)\right]^2}\frac{2n+1}{2\pi n(n+1)}\frac{(n-m)!}{(n+m)!}\times \int_0^{2\pi}\int_0^{\pi} -\mathbf{N}_{\substack{e_{m,n}\\o}}\mathbf{E_{nf}}(r_1,\theta,\phi)\sin\theta d\theta d\phi \quad (13)$$

The Far-Field values are obtained through the weighted coefficients $a_{m,n}$ and $b_{m,n}$, and **M** and **N** vector fields evaluated in a radio belonging to the far zone. In (8) and (9), the limit of the summation must be truncated, so a maximum value for n has been proposed as in [1, 10]:

$$n_{\max} = \kappa\frac{D}{2} \quad (14)$$

where, D is the maximum size of the antenna. For $n>n_{\max}$ the contribution of the elements of the summation is not significant to the value of convergence of the summation. The value of m is bounded by:

$$0 \le m \le n. \quad (15)$$

In addition, for values of m higher than n the associated Legendre function is zero.

Additionally, in order to diminish the sampling error it is recommended that the angular separation between samples (Figure 2) satisfies [11]:

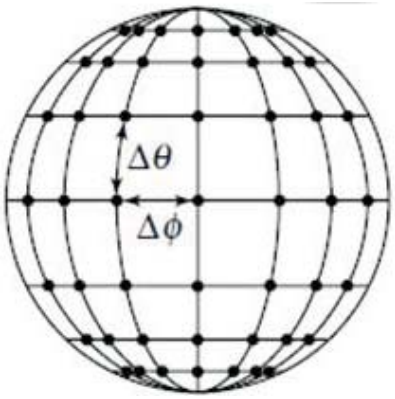

Figure 2. Measurement Grid.

$$\Delta\phi \le \frac{\lambda}{D+2\lambda}, \text{ and, } \Delta\theta \le \frac{\lambda}{D+2\lambda} \quad (16)$$

Finally, it is important to note that NF-FF transformation using spherical wave expansion reduces the truncation errors in the calculation of the weighted coefficients, a and b, because the measurement grid encloses completely the antenna under test. In addition, the probe's compensation becomes unnecessary since the antenna under test and the field probe are always aligned [12, 13]. However, a disadvantage of this technique is that it involves a complex mathematical formulation due to the emergence of Hankel functions and associated Legendre polynomials. For this reason, matrix operations and numerical integration become necessary and the computation time and memory requirements increase.

4. The NF-FF Transformation algorithm

The general outline of the algorithm is shown in Figure 3. The preliminary data refers to the input parameters of the algorithm: the operation frequency, dimensions of the antenna under test, the measurement distance in the Near-Field region and the distance in the Far-Field region where the **M** and **N** vectors will be computed. Then, from the data of the tangential electric field measured in Near-Field the coefficients $a_{m,n}$ and $b_{m,n}$ are calculated. Subsequently, the electric

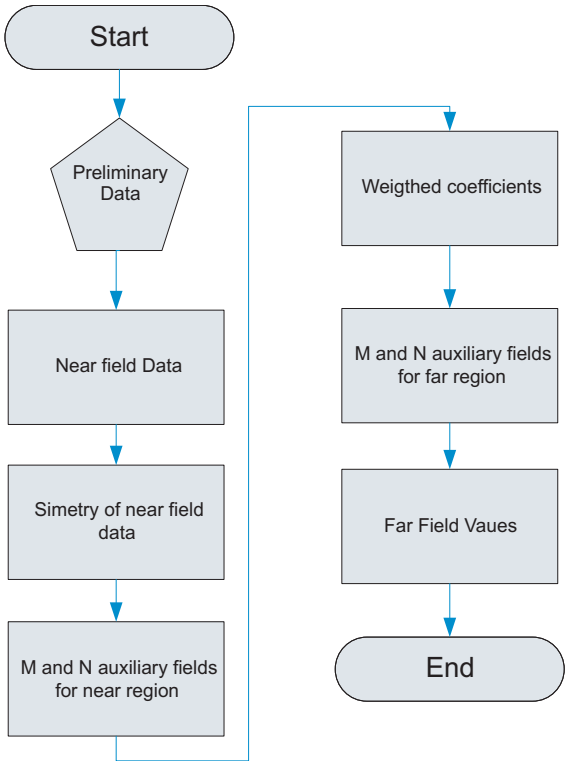

Figure 3. Algorithm Flowchart.

field in Far-Field is computed using the new **M** and **N** vectors corresponding to a distance in the Far-Field region and from the coefficients previously calculated.

5. Experimental procedure

In the experimental procedure was employed the following high-frequency measurement equipments: Vector Network Analyzer (VNA), Multi-Axis Positioning System (MAPS), Multi-Controller (MDC), Anechoic Chamber, Waveguides, Ferrite cable, Alignment Laser, control and data acquisition software. The measurement of electric field in the Fresnel zone must be made of with caution, considering the factors that would imply a distortion in the results. The test procedure is shown in Figure 4, resumed as a flowchart. It is important, in order to reduce errors, to wait until the VNA has reached thermal stabilization. To ensure repeatability of measurements, the relative humidity should be between the ranges recommended by equipment's manufacturers (30-60%). Then, a routine calibration (open, short and match) of the VNA should be performed with the purpose of compensating the

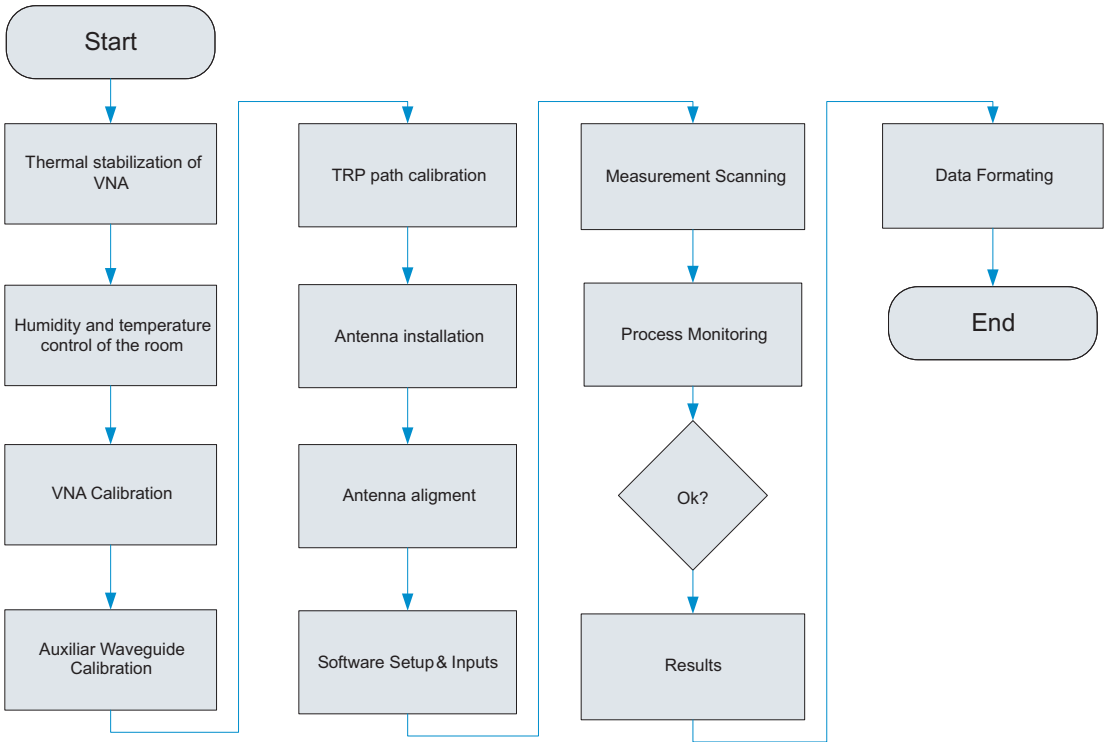

Figure 4. Measurement procedure flowchart.

measurement plane to the antenna input port under test. The total attenuation of the cable paths should be measured in order to calculate the tangential electric field. Finally, the antenna under test should be aligned to the receiving antenna (field probe) using a laser multi axis.

6. Validating tests

Test 1: NF-FF transformation for an infinitesimal dipole

This method consists in the transformation of theoretical electric Near-Field distribution obtained from the equations that describe the electric field in any region of space for an infinitesimal dipole [6]. The aforementioned theoretical equations are given by,

$$\mathbf{E}_\theta = j\eta \frac{I_0 kl \sin\theta}{4\pi r}\left[1+\frac{1}{jkr}-\frac{1}{(kr)^2}\right]e^{-kr}, \text{ and} \quad (17)$$

$$\mathbf{E}_\phi = 0 \quad (18)$$

where I_0 is the current in z direction of the dipole, η is the wave impedance in free space, l is the length of the dipole, r is the distance from the origin of coordinates to the source point and θ is the elevation angle as defined in spherical coordinates.

In order to validate the computer application, the output of the algorithm was compared with the values corresponding to the evaluation of the expressions (17) and (18) for a r in the Far-Field region according to (7). The discrepancy on both results would represent the numerical errors introduced by the code. The length of the measured dipole was 1 cm at 3 GHz and was used an angular resolution of 20° in both azimuthal and elevation angle. The value of r used en Near-Field was 1 cm and in the Far-Field region was 20 m.

Test 2: FF-FF transformation for a Half-wave dipole

This test used as the input for the algorithm, measurements made of in Far-Field region in order to transform it to a larger measurement radius. Both patterns were expected to be similar. In consequence, this experiment was a Far-Field to Far-Field transformation. Certainly, the uncertainty associated to the results includes several contributions (such as instruments resolution, calibration uncertainties and positioning and alignment errors associated with the antenna mounting) besides the numerical error. For this test, a half wavelength dipole was employed at 2.45 GHz using a distance of 5 m in the Far-Field region. An angular resolution of 15° in both azimuthal and elevation angle.

Test 3: NF-FF Full FF transformation for a Half-wave dipole

In the last validation test was used a calibrated half wavelength dipole. The measurements were made of in the Fresnel region the within anechoic chamber and then the transformation was performed using our computer application. The result was compared with the electric Far-Field measured directly from the same dipole in the Far-Field region using the same anechoic chamber. It was used the same Half-wave dipole reported in Test 2. The measurement distance in NF was 0.75 m and 5 m in the Far-Field region. An angular resolution of 15° in both azimuthal and elevation angle was used.

7. Results

Figure 5 shows the FF radiation pattern of an infinitesimal dipole at 3 GHz. Both, the FF pattern from NF calculations using the algorithm and the FF pattern directly evaluated in (17) and (18) were plotted superimposed. As shown, the code is able to reproduce the Far-Field data corresponding to a closed equation data describing a Near-Field region. This simple example also shows that the algorithm introduces a minimum numerical error.

In Figure 6, it is shown both the FF radiation pattern of a half-wave dipole at 2.45 GHz measured at 5 m and the FF radiation pattern transformed at 20 m. As shown, the code reproduces a Far-Field data corresponding to an extreme case, where the data is measured in Far-Field and then the code is also evaluated in the far region. This test demonstrates the code introduces an error due to the sampling spatial grid. The reported error was less than 2 dB for the worst case, corresponding to θ = 15°.

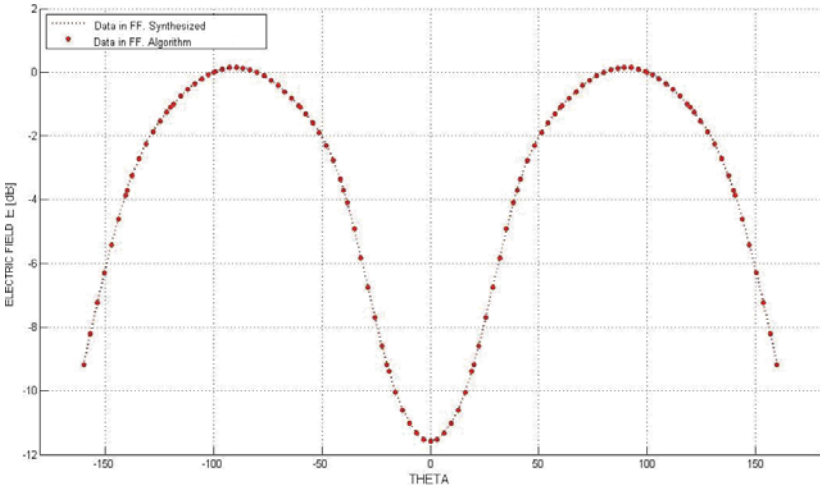

Figure 5. NF-FF transformation for an infinitesimal dipole test result.

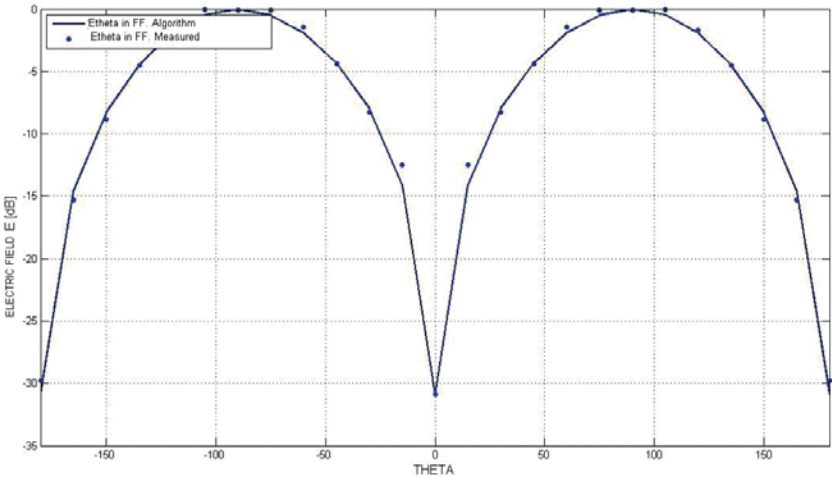

Figure 6. FF-FF transformation for a Half-wave dipole test result.

Figure 7 shows the experimental setup of the third experiment inside the fully anechoic chamber.

In Figure 8, it is shown both the FF radiation pattern of a half-wave dipole at 2.45 GHz measured at 5 m and the FF radiation pattern transformed from the NF measurements made at 0.75 m. This last experiment validates the functionality of the algorithm converting data to the Far-Field region from Near-Field. Table 1 show that maximum error reported was 3 dB in theta 20°.

Finally, some additional results are shown as a complement to this paper in order to verify the functionality of the developed computer ap-

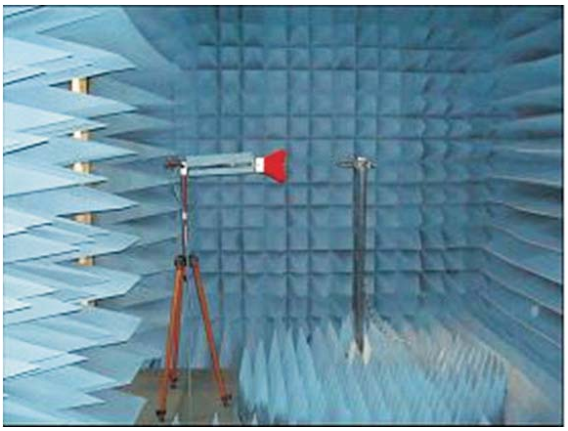

Figure 7. Setup of Near-Field measurement of a half wave length dipole.

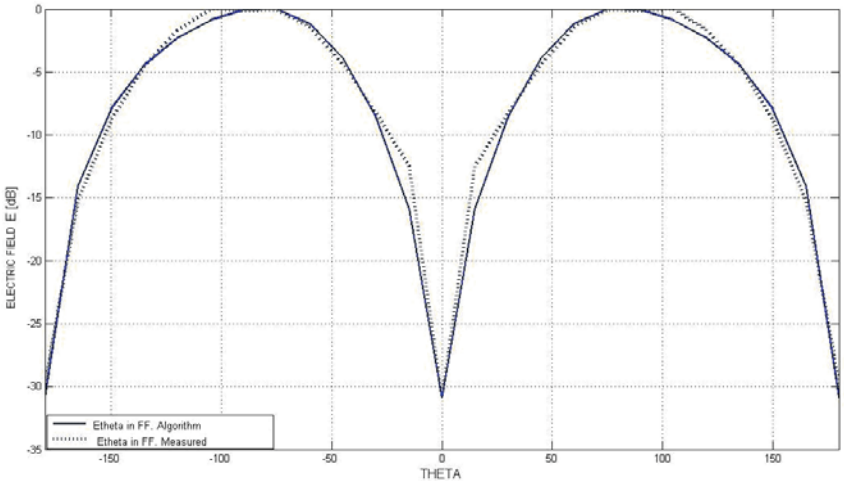

Figure 8. NF-FF transformation for a Half-wave dipole test result.

Table I
Error calculated using a half wavelength dipole measured in Near-Field

Theta [°]	E measured [$dB_{(V/m)}$]	E calculated [$dB_{(V/m)}$]	ΔE [dB]
0	–30,5	–30,7	0,2
10	–22,1	–21,3	–0,8
20	–14,2	–11,2	–3,0
30	–9,1	–8,5	–0,6
40	–5,6	–5,6	0,0
50	–3,4	–3,2	–0,2
60	–1,1	–1,2	0,1
70	–0,5	–0,5	0,0
80	0,2	0,3	–0,1
90	0,1	0,2	–0,1
100	–0,5	0,2	–0,7
110	–1,6	–0,5	–1,1
120	–2,2	–1,8	–0,4

plication. This comparative test consisted in the processing of a Near-Field data provided by the TSC Group from UPC, Barcelona. The electric Near-Field data corresponds to a waveguide slotted antenna at 9.63 GHz, the maximum antenna dimension was 19.17 cm and the measurement distance was 5.35 m. The results are shown in Figure 9, 10 and 11 using the third Ludwig convention [14].

8. Conclusions

It has been developed an algorithm that receives as input the values of tangential electric field measurements on a spherical surface in the Near-Field or Far-Field zone, and from these data, calculates the values of electric field in the Far-Field zone using the spherical wave expansion technique. For this purpose the results were

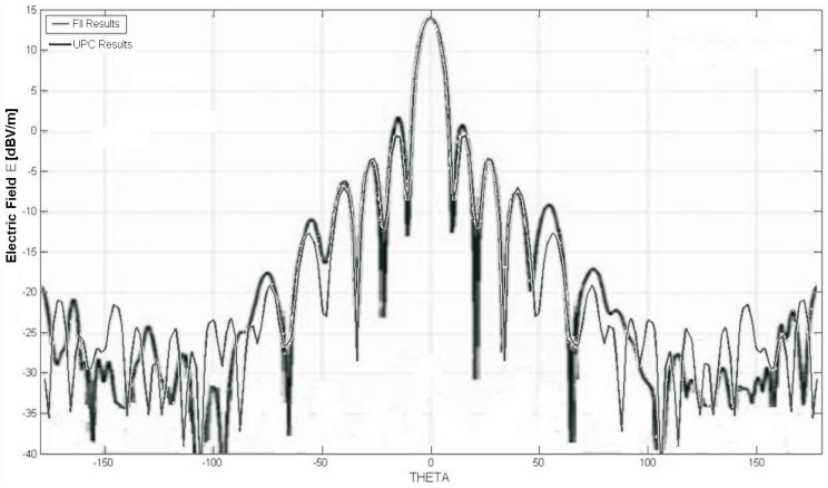

Figure 9. Copolar Electric field in Phi = 0°.

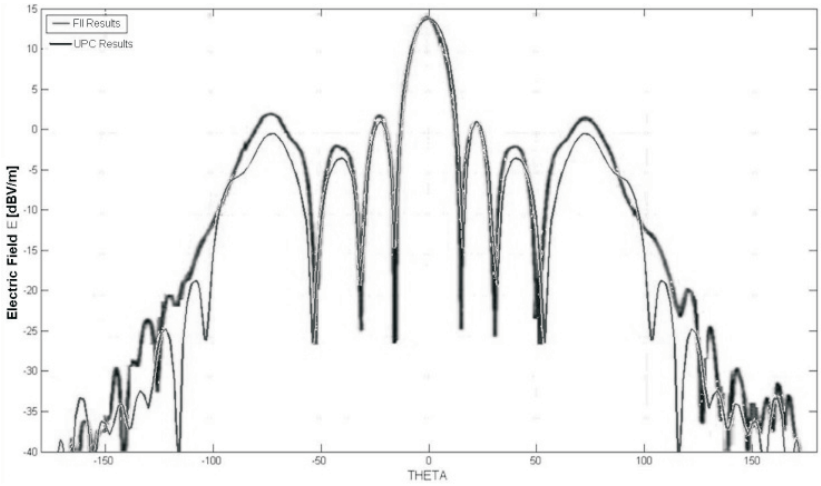

Figure 10. Copolar Electric field in Phi = 45°.

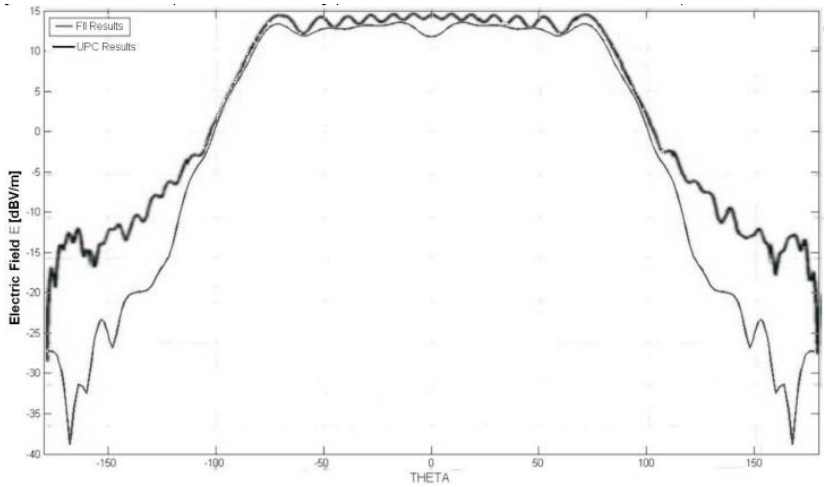

Figure 11. Copolar Electric field in Phi = 90°.

validated using three experimental tests. The first experiment shows the amount of numerical errors using data obtained evaluating theoretical formulation. From the results of the second experiment, we conclude that the numerical error introduced by the algorithm is small, even in some cases could be considered negligible. In addition to this exercise, is verified that the expansion wave is a method capable to calculate the field in any region.

The quality of the data measured in the nearby area plays an important role in the accuracy of the results. It was observed in the third experiment that if the Near-Field data is corrupted, either by noise, multipath reflections, links parasites or any other cause the results obtained by the algorithm may diverge from reality seriously.

Acknowledgements

Special thanks to Dr. Alfonso Zozaya by their valuables contributions in electromagnetic theory during this development and to Dr. Jordi Romeu and Dr. Sebastian Blanch, from UPC, Barcelona, for providing us valuable data file.

References

1. Ludwig, Arthur C. "Near-Field Far-Field Transformation Using Spherical-Wave Expansions. IEEE Transactions on Antennas and Propagation, Vol. AP-19, No. 2, marzo (1971) 2.1, 2.5.3, 5.
2. Pierri, Rocco; D'Elia, Giuseppe; Soldovieri, Francesco. "A Two Probes Scanning Phaseless Near-Field Far-Field Transformation Technique". IEEE Transactions on Antennas and Propagation, Vol. AP-47, No. 5, mayo (1999).
3. Trzaska, Hubert. "Electromagnetic Field Measurements In The Near Field". Atlanta. Noble Publishing, 2001. 2.6
4. Yaghjian, A. D.: "An Overview of Near-Field Antenna Measurements", IEEE Transactions on Antennas and Propagation, Vol. AP-34, No. 1 (1986).
5. Sarkar, T. K., Petre, P., Taaghol, A. and Harrington R. F.: "An Alternative Spherical Near-Field to Far-Field Transformation", Progress in Electromagnetic Research, Vol. 16 (1997), 269-286.
6. Balanis, C. A. "Antenna Theory. Analysis and Design", John Wiley & Sons, New Jersey, 2005. 2.2, 2.5, 2.8, 3.2, 4.1.
7. Bucci, Ovidio; D'Elia, Giuseppe; Leone, Giovanni; Pierri, Rocco. "Far-Field Pattern Determination from the Near-Field Amplitude on Two Surfaces". IEEE Transactions on Antennas and Propagation, vol. AP-38, No. 11, noviembre 1990. 1.1, 2.1
8. Bucci, Ovidio; D'Elia, Giuseppe; Migliore, Marco. An Efective Near-Field Far-Field Transformation Technique from Truncated and Inaccurate Amplitude-Only Data. IEEE Transactions on Antennas and Propagation, Vol. AP-47, No. 9, septiembre 1999. 2.1
9. Bucci, Ovidio; Gennarelli, Claudio. Use of Sampling Expansions in Near-Field Far-Field Transformation: The Cylindrical Case. IEEE Transactions on Antennas and Propagation, Vol. AP-36, No. 6, junio 1988. 3.1
10. [10] P. D. Potter, "Application of spherical wave theory to Cassegrainian-fed paraboloids", IEEE Trans. Antennas Propagat.,Vol. AP-15, Nov. 1967, pp. 727-736.
11. Yaghjian, Arthur D. An Overview of Near-Field Antenna Measurements. IEEE Transactions on Antennas and Propagation, Vol. AP-34, No. 1, enero 1986. 2.1, 2.6.1, 2.6.2.
12. Stratton, Julius A. Electromagnetic Theory. Wiley and Interscience, 2007. 2.4.1, 2.4.1,
13. Schmidt, Carsten; Leibfritz, Martin; Eibert, Thomas. Fully Probe-Corrected Near-Field Far-Field Transformation Employing Plane Wave Expansion and Diagonal Translation Operators. IEEE Transactions on Antennas and Propagation, Vol. AP-56, No. 3, marzo (2008)
14. Ludwig, A. C., "The Definition of Cross Polarization", IEEE Transactions on Antennas and Propagation, pp 116-119 (1973).

Recibido el 7 de Abril de 2011
En forma revisada el 16 de Enero de 2012